Development and Validation of N-nitrosamine Rejection Mathematical Model Using a Spiral-wound Reverse Osmosis Process

Mudhar. A. Al-Obaidi, Chakib Kara-Zaïtri, Iqbal. M. Mujtaba*

Chemical Engineering Division, School of Engineering, University of Bradford, Bradford, West Yorkshire BD7 1DP, UK
I.M.Mujtaba@bradford.ac.uk

In this paper, a one-dimensional mathematical model based on coupled differential and algebraic equations has been developed for analysing the separation mechanism of a N-nitrosamine in a spiral-wound reverse osmosis process. The model is based on Spiegler and Kedem's work on mass transport and Darcy's law and concentration polarization to analyse the pressure drop and mass transfer coefficient in the module feed channel respectively. The model is built using the gPROMS software suite and validated using N-nitrosamine rejection experimental data from the literature, obtained by using a pilot-scale cross-flow reverse osmosis filtration system. Analysis results derived from the model corroborate experimental data.

1. Introduction

Reverse Osmosis (RO) is a water purification process, used in in water desalination and waste treatment that uses a semipermeable membrane to remove undesirable particles. RO has many immediate advantages including minimum thermal damage, high packing density and lower energy consumption (Reverberi et al., 2014) . Furthermore, spiral-wound RO modules are less susceptible to membrane fouling and are easier to clean (Song, 2002). With the increasing application of RO in the removal of organic compounds, the modelling of membrane separation and mass transport mechanisms constitutes a significant factor in the development of cost effective and optimum design strategies. Various types of models have been proposed to describe the transport phenomena of solvent and solute through the membrane. These models are based on the three-parameter irreversible thermodynamics model (Spiegler and Kedem, 1966), the solution-diffusion model (Lonsdale et al., 1965) and the pore flow models (Jonsson and Boesen, 1975). Successful examples of membrane transport mechanisms based on the Spiegler and Kedem model have been well described in the literature and validated for both wastewater treatment and seawater desalination processes. For example, Ahmad et al. (2007) have developed a model suitable for the multiple solutes system for unsteady-state simulation and prediction of membrane filtration dynamics in terms of permeate flux and concentration of each solute. This model was validated with experimental data derived from pre-treated palm oil mill effluent as a feed using a PVDF hollow fibre membrane module in a pilot plant scale RO system. Whereas, Mane et al. (2009) have studied boron rejection using two commercially spiral-wound modules in pilot-scale and full-scale RO processes by varying pH and pressures. Patroklou et al. (2013) developed a mathematical model of RO for boron rejection and validated the model using experimental data of Mane et al. (2009).

To the best of authors' knowledge, the development of a spiral-wound RO model based on the Spiegler and Kedem concept and its validation of N-nitrosamine compounds have only been conducted by Fujioka et al. (2014). Their model has conidered the variation of operating parameters in the *x- axis* with assuming zero permeate pressure. The aim of this paper is to develop a new distributed model with relaxing the proposed assumption of zero pressure at the permeate side. The new idea here is to develop a mathematical steady state model based on the work by Spiegler and Kedem to simulate the rejection of N-nitrosamine compounds using a spiral-wound RO filtration process. The model will account for the spatial variation of all operating parameters along the length of the feed and permeate channels of the module (distributed model). The

validation of this model has been corroborated against experimental data derived from the literature. The data includes uncharged N-nitrosamine compounds rejection based on a pilot-scale plant of three cylindrical pressure vessels with spiral-wound elements. The process model developed can be used later to study the variation of solute concentration, pressure, flow rate, solvent and solute fluxes along the length of the feed channel and to investigate the impact of variation in operating conditions on the unit performance.

2. Model Rationale and Development

2.1 The Assumptions
The following assumptions are made to develop the proposed process model:
1. Spiegler and Kedem's model is used for mass transport through the module.
2. The membrane characteristics and the channel geometries are assumed constant.
3. Validity of Darcy's law where the friction parameter is used to characterize the pressure drop in both the feed and permeate channels.
4. Constant solute concentration in the permeate channel and the average value will be calculated from the inlet and outlet calculated concentrations.
5. The underlying process is assumed to be isothermal.

2.2 Governing Equations
The water and solute fluxes ($J_{w(x)}$, $J_{s(x)}$) (m/s, kmol/m² s) can be calculated using Spiegler and Kedem's (1966) model:

$$J_{w(x)} = L_p \left(\Delta P_{b_{(x)}} - \sigma \, \Delta \pi_{s(x)} \right) \tag{1}$$

$$J_{s(x)} = J_{w(x)} \, (1 - \sigma) \, C^{\sim}_{b(x)} + \omega \, \Delta \pi_{s(x)} \tag{2}$$

Where, $L_p, \Delta P_{b_{(x)}}, \sigma, \Delta \pi_{s(x)}$ and ω are solvent transport coefficient (m/atm s), trans-membrane pressure (atm), the reflection coefficient (*dimensionless*), the osmotic pressure difference (atm) and the solute permeability coefficients of the membrane (kmol/m²s atm) respectively. While, ($C^{\sim}_{b(x)}$) (kmol/m³) is the mean solute concentration in the feed side along the x-axis and calculated by.

$$C^{\sim}_{b(x)} = \frac{C_{b(x)} - C_{p(av)}}{ln \left(\frac{C_{b(x)}}{C_{p(av)}} \right)} \tag{3}$$

Where, $C_{b(x)}$ and $C_{p(av)}$ are feed solute concentration and the average permeate concentration (Kmol/m³) respectively. The following two equations work well for solute flux and the difference of osmotic pressure:

$$J_{s(x)} = J_{w(x)} \, C_{p(av)} \tag{4}$$

$$\Delta \pi_{s(x)} = R \, T_b \, (C_{w(x)} - C_{p(av)}) \tag{5}$$

Where, R, T_b and $C_{w(x)}$ ($\frac{atm \, m^3}{°K \, Kmol}$, °C, $\frac{Kmol}{m^3}$) are the gas constant, the brine temperature and the molar solute concentration on the membrane surface respectively. Substitute Eq(5) in Eqs(1) and (2) gives:

$$J_{w(x)} = L_p \left(\Delta P_{b_{(x)}} - \sigma \, R \, T_b \, (C_{w(x)} - C_{p(av)}) \right) \tag{6}$$

$$J_{s(x)} = J_{w(x)} \, (1 - \sigma) \, C^{\sim}_{b(x)} + \omega \, R \, T_b \, (C_{w(x)} - C_{p(av)}) \tag{7}$$

Re-arrangement Eq(7) yields.

$$C_{w(x)} - C_{p(av)} = \frac{J_{w(x)} \, C_{p(av)}}{\omega \, R \, T_b} - \frac{C^{\sim}_{b(x)} \, (1 - \sigma) \, J_{w(x)}}{\omega \, R \, T_b} \tag{8}$$

Then, substituting ($C_{w(x)} - C_{p(av)}$) in Eq(6) with re-arrangements gives:

$$J_{w(x)} = \frac{L_p \, \Delta P_{b(x)}}{1 + \frac{\sigma \, C_{p(av)} \, L_p}{\omega} - \frac{C^{\sim}_{b(x)}(1 - \sigma) \, \sigma \, L_p}{\omega}} \tag{9}$$

Eq(9) can be simplified to:

$$J_{w(x)} = \frac{L_p \, \Delta P_{b(x)}}{\emptyset_{(x)}} \qquad \text{where,} \qquad \emptyset_{(x)} = 1 + \frac{\sigma \, C_{p(av)} \, L_p}{\omega} - \frac{C^{\sim}_{b(x)}(1 - \sigma) \, \sigma \, L_p}{\omega} \tag{10}$$

The trans-membrane pressure ($\Delta P_{b(x)}$) (atm) is related the pressure in both the feed and permeate channels.

$$\Delta P_{b(x)} = P_{b(x)} - P_{p(x)} \tag{11}$$

Where, $P_{b(x)}$ and $P_{p(x)}$ are feed and permeate pressures (atm) respectively. The variation of trans-membrane pressure along x-axis can be calculated from:

$$\frac{d \, \Delta P_{b(x)}}{dx} = \frac{d \left(P_{b(x)} - P_{p(x)} \right)}{dx} \tag{12}$$

Specifically, the mass balance in both channels can be written as:

$$F_{b(0)} = F_{b(x)} + F_{p(x)} \tag{13}$$

$F_{b(0)}$, $F_{b(x)}$ and $F_{p(x)}$ (m³/s) are feed flow rate at x = 0 and at any point along the x-axis and permeate flow rate respectively. Also, Darcy's law can be used to describe the drop of pressure in both channels (Assumption 3).

$$\frac{dP_{b(x)}}{dx} = -b\, F_{b(x)} \tag{14}$$

$$\frac{dP_{p(x)}}{dx} = -b\, F_{p(x)} \tag{15}$$

Where, b (atm s/m⁴) is Feed and permeate channels friction parameter. The substitution of Eqs(14) and (15) in Eq(12), gives:

$$\frac{d\,\Delta P_{b(x)}}{dx} = -b\,(F_{b(x)} - F_{p(x)}) \tag{16}$$

While, the derivation of Eq(13) with the *x-axis*, gives:

$$\frac{dF_{b(x)}}{dx} = -\frac{dF_{p(x)}}{dx} = -W\, J_{w(x)} \tag{17}$$

Where, W (m) is the width of membrane. Then, dividing Eqs(16) and (17), gives:

$$\frac{d\,\Delta P_{b(x)}}{dF_{b(x)}} = \frac{b(F_{b(x)} - F_{p(x)})}{W\, J_{w(x)}} \tag{18}$$

The proposed correlations of Koroneos (2007) to calculate the physical properties of seawater (density, viscosity and diffusion coefficient) are considered identical to the analysis of dilute aqueous solutions of wastewater. Finally, the re-arrangement and integration yields the specific equations of the model used for simulation as follows:

The feed flow rate ($F_{b(x)}$) (m³/s) at any point along the x-axis is calculated by:

$$F_{b(x)}^2 = F_{b(0)}^2 + \frac{W\, L_p}{b\, \emptyset_{(x)}}\left(\Delta P_{b(x)}^2 - \Delta P_{b(0)}^2\right) + 2\left(F_{b(0)} - F_{b(x)}\right)\left(F_{b(x)} - F_{b(0)}\right) \tag{19}$$

The feed pressure ($P_{b(x)}$) (*atm*) and the trans-membrane pressure ($\Delta P_{b(x)}$) (*atm*) are calculated by Eqs(20, 21):

$$P_{b(x)}^2 = \left[P_{b(0)} - \left(b\, x\, F_{b(0)}\right) - \left(b\, x\, \left(\frac{W\, L_p}{b\, \emptyset_{(x)}}\right)^{0.5}\left(\Delta P_{b(x)} - \Delta P_{b(0)}\right)\right)\right]^2 - \left[b^2\, x^2\left(2\left(F_{b(0)} - F_{b(x)}\right)\left(F_{b(x)} - F_{b(0)}\right)\right)\right] \tag{20}$$

$$\Delta P_{b(x)}^2 = \left[\Delta P_{b(0)} - \left(b\, x\, F_{b(0)}\right) - \left(b\, x\, \left(\frac{W\, L_p}{b\, \emptyset_{(x)}}\right)^{0.5}\left(\Delta P_{b(x)} - \Delta P_{b(0)}\right)\right)\right]^2 - \left[b^2\, x^2\left(2\left(F_{b(0)} - F_{b(x)}\right)\left(F_{b(x)} - F_{b(0)}\right)\right)\right] + \left[b^2\, x^2\left(F_{b(0)} - F_{b(x)}\right)^2\right] \tag{21}$$

The water flux ($J_{w(x)}$) (*m/sec*) and solute flux ($J_{s(x)}$) (*kmol/m² s*) depict in the counter of Eqs(22 and 23).

$$J_{w(x)} = \frac{L_p}{\emptyset_{(x)}}\left\{\Delta P_{b(0)} - \left(b\, x\, F_{b(0)}\right) - \left(b\, x\, \left(\frac{W\, L_p}{b\, \emptyset_{(x)}}\right)^{0.5}\left(\Delta P_{b(x)} - \Delta P_{b(0)}\right)\right) - \left[b\, x\left(2\left(F_{b(0)} - F_{b(x)}\right)\left(F_{b(x)} - F_{b(0)}\right)\right)^{0.5}\right] + \left[b\, x\left(F_{b(0)} - F_{b(x)}\right)\right]\right\} \tag{22}$$

$$J_{s(x)} = \left(J_{w(x)}\,(1 - \sigma)\, C_{\widetilde{b}(x)}\right) + \left(\omega\, R\, T_b\,\left(C_{b(x)} - C_{p(av)}\right) e^{\frac{J_{w(x)}}{k_{(x)}}}\right) \tag{23}$$

Eq(24) is used to calculate the feed solute concentration along the x-axis ($C_{b(x)}$) (*kmol/m³*) (Lee et al., 2010).

$$\frac{d\frac{\left(C_{b(x)}\, F_{b(x)}\right)}{t_f\, W}}{dx} = -\frac{J_{w(x)}\, C_{p(av)}}{t_f} + \frac{J_{w(x)}\, C_{b(x)}}{t_f} + \frac{d}{dx}\left(D_{b(x)}\frac{dC_{b(x)}}{dx}\right) \tag{24}$$

D_b is the diffusivity parameter of feed (*m²/s*). Then, the permeate flow rate ($F_{p(x)}$) (*m³/s*) is calculated by:

$$F_{p(x)}^2 = F_{p(0)}^2 + \left(\frac{W\, L_p\, x}{\emptyset_{(x)}}\Delta P_{b(0)}\right)^2 - \left(\frac{W\, L_p\, b}{\emptyset_{(x)}} F_{b(0)}\left(\frac{x^2}{2}\right)\right)^2 - \left\{\left(\frac{W\, L_p}{\emptyset_{(x)}}\right)^{1.5} b^{0.5}\left(\frac{x^2}{2}\right)\left(\Delta P_{b(x)} - \Delta P_{b(0)}\right)\right\}^2 - \left\{\left(\frac{W\, L_p\, b}{\emptyset_{(x)}}\right)\left(\frac{x^2}{2}\right)\left(2\left(F_{b(0)} - F_{b(x)}\right)\left(F_{b(x)} - F_{b(0)}\right)\right)^2\right\} + \left(\left(\frac{W\, L_p\, b}{\emptyset_{(x)}}\right)\left(\frac{x^2}{2}\right)\left(F_{b(0)} - F_{b(x)}\right)\right)^2 \tag{25}$$

The variation of permeate pressure along the x-axis is calculated according to Eq(26).

$$P_{p(x)}^2 = P_{p(0)}^2 - \left(b\,x\,F_{b(0)}\right)^2 - \left(\left(\frac{W\,L_{p\,b}}{\emptyset_{(x)}}\right)\left(\frac{x^2}{2}\right)\Delta P_{b(0)}\right)^2 + \left(\left(\frac{W\,L_p}{\emptyset_{(x)}}\right)\left(\frac{x^3}{6}\right)b^2\,F_{b(0)}\right)^2 +$$

$$\left[b^{1.5}\left(\frac{x^3}{6}\right)\left(\frac{W\,L_p}{\emptyset_{(x)}}\right)^{1.5}\left(\Delta P_{b(x)} - \Delta P_{b(0)}\right)\right]^2 + \left(b^2\left(\frac{W\,L_p}{\emptyset_{(x)}}\right)\left(\frac{x^3}{6}\right)\left(2\left(F_{b(0)} - F_{b(x)}\right)\left(F_{b(x)} - F_{b(0)}\right)\right)\right)^2 - \qquad (26)$$

$$\left(\left(\frac{x^3}{6}\right)\left(\frac{W\,L_{p\,b}}{\emptyset_{(x)}}\right)\left(F_{b(0)} - F_{b(x)}\right)\right)^2$$

The mass transfer coefficient $(k_{(x)})$ (m/s) and feed velocity are calculated using Eqs(27 and 28).

$$k_{(x)} = 0.753\left(\frac{K}{2-K}\right)^{0.5}\left(\frac{D_{b(x)}}{t_f}\right)\left(\frac{\mu_{b(x)}\,\rho_{b(x)}}{D_{b(x)}}\right)^{0.1666}\left(\frac{2\,t_f{}^2\,U_{b(x)}}{D_{b(x)}\,\Delta L}\right)^{0.5} \qquad (27)$$

$$U_{b(x)} = F_{b(x)}\,/\,(t_f\,W) \qquad (28)$$

Where, $K, \mu_{b(x)}, \rho_{b(x)}$ and $U_{b(x)}$ are the efficiency of mixing ($K = 0.5$) *(dimensionless)*, feed viscosity (*Kg/m sec*), density (*kg/m³*) and feed velocity (*m/sec*) respectively (Mane et al., 2009). The concentration at the wall membrane ($C_{w(x)}$) (*kmol/m³*) is calculated using Eq(29).

$$\frac{C_{w(x)} - C_{p(av)}}{C_{b(x)} - C_{p(av)}} = \exp\left(\frac{J_{w(x)}}{k_{(x)}}\right) \qquad (29)$$

Eqs(30, 31 and 32) have been used to calculate the permeate solute concentrations ($C_{p(x)}$) (*kmol/m³*) at both x = 0 and x = L and the average permeate concentration ($C_{p(av)}$) (*kmol/m³*) respectively.

$$C_{p(0)} = \frac{B_s\,R\,T_b\,C_{b(0)}\,e^{\frac{J_{w(0)}}{k_{(0)}}}}{J_{w(0)} + B_s\,R\,T_b\,e^{\frac{J_{w(0)}}{k_{(0)}}}} \qquad (30)$$

$$C_{p(L)} = \frac{B_s\,R\,T_b\,C_{b(L)}\,e^{\frac{J_{w(L)}}{k_{(L)}}}}{J_{w(L)} + B_s\,R\,T_b\,e^{\frac{J_{w(L)}}{k_{(L)}}}} \qquad (31)$$

$$C_{p(av)} = \frac{C_{p(0)} + C_{p(L)}}{2} \qquad (32)$$

B_s is solute transport coefficient (*m/s*) used for the case of assuming ($\sigma = 1$) as can be found in the solution-diffusion model. Finally, Eq(33 and 34) are used to calculate the solute rejection and total water recovery (*dimensionless*).

$$Rej = \frac{C_{b(L)} - C_{p(av)}}{C_{b(L)}} \times 100 \qquad (33)$$

$$Rec_{(Total)} = \frac{F_{p(Total)}}{F_{b(0)}} \times 100 \qquad (34)$$

The model equations have been solved using the gPROMS software where the filtration channel is divided into a number of segments of equal intervals (Δx). For a given inlet feed flow rate, pressure, solute concentration and temperature with a guesstimate of the initial value of permeate pressure (close to 1 atm), the proposed model can predict the longitudinal variation of all parameters in the feed and permeate channels in the x-axis by using the estimated values of membrane transport parameters L_p, B_s, ω, σ and b.

3. Materials and methods

A pilot-scale RO filtration system of three 4 inch glass-fiber pressure vessels was used by Fujioka et al. (2014) in the experiments (described below) of eight N-nitrosamine solutes rejection with a molecular weight in the range of (74 – 158 g/mol) as summarized in Table 1. The N-nitrosamine stock solution contains 10 mg/L of each uncharged N-nitrosamine solutes in the tested solution (pH 8) [N-nitrosodimethylamine-D6 (NDMA), N-nitrosomethylethylamine-D3 (NMEA), N-nitrosopyrrolidine-D8 (NPYR), N-nitrosodiethylamine-D10 (NDEA), N-nitrosopiperidine-D10 (NPIP), N-nitrosomorpholine-D8 (NMOR), N-nitrosodipropylamine-D14 (NDPA) and N-nitrosodi-n-butylamine-D9 (NDBA)] were prepared in pure methanol. Also, an aqueous feed of stock solutions of NaCl, CaCl$_2$ and NaHCO$_3$ were also prepared in Milli-Q water at 2 M (NaCl) and 0.1 M (CaCl$_2$ and NaHCO$_3$) to simulate the electrolyte composition typically found in treated wastewater. Then, the filtration experiments were carried out by introducing the stock solution of N-nitrosamine compounds in the feed to obtain approximately (250 ng/L) of each target Nitrosamine compound. Each pressure vessel holds only one spiral-wound element. The pressure vessels are connected in series where the concentrated feed solution of the first vessel was transferred to the second vessel followed by the third one. The permeate is then collected from the stages and recycled back with the retentate solution into the feed tank to maintain constant feed concentration.

The feed was pumped at constant volumetric flow rate of 2.43×10^{-3} (m³/s), while the average permeate flux was adjusted at 2.78×10^{-6}, 5.56×10^{-6} and 8.33×10^{-6} (m/s) during the experiments by increasing the operating feed pressure from 4, 6.5 and 10.1 atm respectively. The feed temperature was controlled at 20 ± 0.1 °C along the experiments.

Table 1: Physical and transport parameters of the selected N-nitrosamines (Fujioka et al., 2014)

Name	Molecular weight (g/mol)	Permeability coefficient, B_s (m/s)	Water permeability coefficient, (L_p) (m/s atm) at 20 °C	Reflection coefficient, σ (dimensionless)
NDMA	74.05	4.75×10^{-6} - 5.35×10^{-6}	1.06×10^{-6} – 1.27×10^{-6}	0.951 - 0.985
NEMA	88.06	1.15×10^{-6} - 1.23×10^{-6}	1.05×10^{-6} – 1.21×10^{-6}	0.936 – 0.989
NPYR	100.06	4.18×10^{-7} - 4.39×10^{-7}	1.05×10^{-6} – 1.23×10^{-6}	0.983 – 0.998

4. Determination of Transport Parameters

Unknown parameters of the membrane elements and the operating conditions should be determined before solving the model equations. In the simulation study, experimental data will be used to predict the best values of unknown parameters, which are then used with the known parameters to check the behavior of the unit with the variance of operating variables. The friction and the model transport parameters for each run was calculated using gEST parameter estimation in gPROMS software using the experiments conducted by Fujioka et al. (2014). The registered values of friction parameter are (62, 194 and 395 (atm s/m⁴)) for the average permeate fluxes 2.78×10^{-6}, 5.56×10^{-6} and 8.33×10^{-6} (m/s) respectively. The membrane transport parameters of the three selected N-nitrosamine solutes (NDMA, NEMA and NPYR) were obtained from the experiments conducted by Fujioka et al. (2014) and listed in Table 1. Also, the specifications of the spiral-wound membrane element can be shown in Table 2.

Table 2: Specifications of the spiral-wound membrane element

Make	Hydranautics, Oceanside, CA., USA
Membrane type and configuration	ESPA2-4040, Spiral-wound, Composite Polyamide
Feed and permeate spacer thickness (t_f) and (t_p), (m)	6.6×10^{-4}
Membrane sheet area, (m^2)	7.9
Membrane sheet length (L) and width (W) (m)	0.9 and 8.7778

5. Model validation

The model described in section 2 has been validated by comparing the model predictions results with those obtained from actual experimentation for the specific RO membrane. Figure 1 shows the comparison of model rejections of the three selected N-nitrosamines at three different overall permeate fluxes against experimental results. The clear corroboration with experimental data readily shows the suitability of the model to measure the observed rejection data with an accepted error within high operating pressures. Furthermore, Figure 1 shows that the model can be used to simulate the observed data at low operating pressure (low average permeate flux) but with some minor deviation. This might be attributed to the inaccurate estimation of the transport membrane parameters at such pressure.
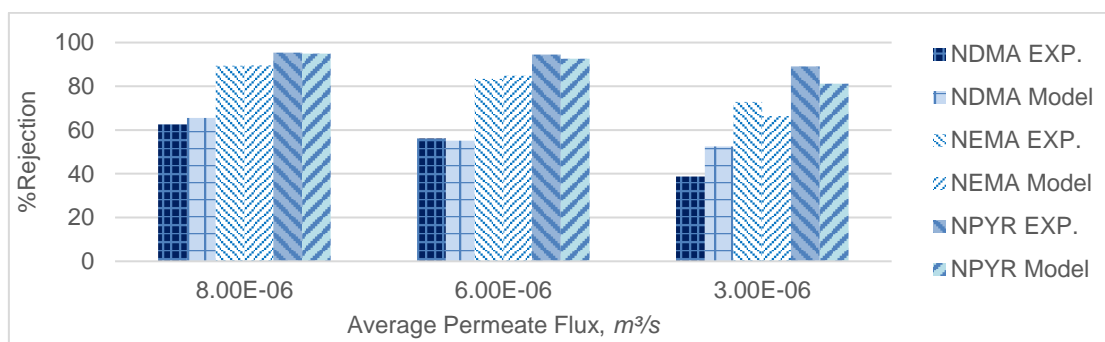

Figure 1: Experimental and model rejections of NDMA, NEMA and NDEA with average permeate flux

In addition, Figures 2 and 3 show the linear fittings with a regression coefficient R² (close to 1) for both the experimental and model prediction of the outlet feed flow rate and pressure respectively.
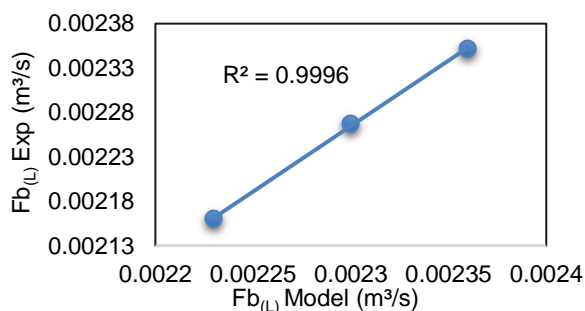

Figure 2: Linear fitting of experimental and model prediction of outlet feed flow rate
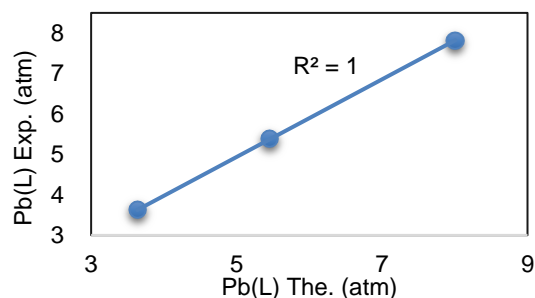
Figure 3: Linear fitting of experimental and model prediction of outlet feed pressure

6. Conclusions

A steady state one-dimensional mathematical model based on the work of the Spiegler and Kedem has been developed for a spiral-wound reverse osmosis process. The model has been validated using a simulation study with experimental data derived from N-nitrosamine compounds rejection. Analysis results readily show that the proposed model can be used to simulate wastewater rejection during scale-plant design with an accepted convergence for most operating parameters. Further work is planned to examine the impact of the operating variables on N-nitrosamine rejection.

References

Ahmad A. L., Chong M. F. and Bhatia S., 2007, Mathematical modelling of multiple solutes system for reverse osmosis process in palm oil mill effluent (POME) treatment. Chemical Engineering Journal, 132, 183-193.

Fujioka T., Khan S. J., Mcdonald J. A., Roux A., Poussade Y., Drewes J. E. and Nghiem L. D., 2014, Modelling the rejection of N-nitrosamines by a spiral-wound reverse osmosis system: Mathematical model development and validation. Journal of Membrane Science, 454, 212-219.

Jonsson G. and Boesen C. E., 1975, Water and solute transport through cellulose acetate reverse osmosis membranes. Desalination, 17, 145-165.

Koroneos C., Dompros A. and Roumbas G., 2007, Renewable energy driven desalination systems modelling. Journal of Cleaner Production, 15, 449-464.

Lee C., Chen Y. and Wang G., 2010, A dynamic simulation model of reverse osmosis desalination systems. The 5th International Symposium on Design, Operation and Control of Chemical Processes, PSE ASIA, Singapore.

Lonsdale H. K., Merten U. and Riley R. L., 1965, Transport properties of cellulose acetate osmotic membranes. Journal of Applied Polymer Science, 9, 1341-1362.

Mane P. P., Park P.-K., Hyung H., Brown J. C. and Kim J.-H., 2009, Modelling boron rejection in pilot- and full-scale reverse osmosis desalination processes. Journal of Membrane Science, 338, 119-127.

Patroklou G., Sassi, K.M. and Mujtaba, I.M., 2013, Simulation of boron rejection by seawater reverse osmosis desalination. Chemical Engineering Transaction, 32, 1873-1878.

Reverberi A., Fabiano B., Cerrato C. and Dovì V., 2014, Concentration polarization in reverse osmposis membranes: Effect of membrane splitting. Chemical Engineering Transaction, 39, 763-768.

Song L., Hong S., Hu J., Ong S. and Ng W., 2002, Simulations of Full-Scale Reverse Osmosis Membrane Process. Journal Of Environmental Engineering, 128, 10, 960.

Spiegler K. S. and Kedem O., 1966, Thermodynamics of hyperfiltration (reverse osmosis): criteria for efficient membranes. Desalination, 1, 311-326.